



RESEARCH ARTICLE

Nonviral overexpression of Scleraxis or Mohawk drives reprogramming of degenerate human annulus fibrosus cells from a diseased to a healthy phenotype

Shirley Tang¹  | Connor Gantt¹ | Ana Salazar Puerta¹ | Lucy Bodine² | Safdar Khan³ | Natalia Higueta-Castro¹ | Devina Purmessur^{1,3} 

¹Department of Biomedical Engineering, The Ohio State University, Columbus, Ohio, USA

²Department of Mechanical Engineering, The Ohio State University, Columbus, Ohio, USA

³Department of Orthopedics, The Ohio State University Wexner Medical Center, Columbus, Ohio, USA

Correspondence

Devina Purmessur, Department of Biomedical Engineering, The Ohio State University, 3016 Fontana Laboratories, 140 W, 19th Avenue, Columbus, OH 43210, USA.
Email: purmessurwalter.1@osu.edu

Natalia Higueta-Castro, Department of Orthopedics, The Ohio State University Wexner Medical Center, 3002 Fontana Laboratories, 140 W, 19th Avenue, Columbus, OH 43210, USA.
Email: higuitacastro.1@osu.edu

Funding information

National Institute of Arthritis and Musculoskeletal and Skin Diseases, Grant/Award Numbers: 1R01AR079485-01, R61 AR076786; Orthopaedic Research Society, Grant/Award Number: ON Foundation/ORS Kickstarter Grant

Abstract

Background: Intervertebral disc (IVD) degeneration is a major contributor to low back pain (LBP), yet there are no clinical therapies targeting the underlying pathology. The annulus fibrosus (AF) plays a critical role in maintaining IVD structure/function and undergoes degenerative changes such as matrix catabolism and inflammation. Thus, therapies targeting the AF are crucial to fully restore IVD function. Previously, we have shown nonviral delivery of transcription factors to push diseased nucleus pulposus cells to a healthy phenotype. As a next step in a proof-of-concept study, we report the use of Scleraxis (SCX) and Mohawk (MKX), which are critical for the development, maintenance, and regeneration of the AF and may have therapeutic potential to induce a healthy, pro-anabolic phenotype in diseased AF cells.

Methods: MKX and SCX plasmids were delivered via electroporation into diseased human AF cells from autopsy specimens and patients undergoing surgery for LBP. Transfected cells were cultured over 14 days and assessed for cell morphology, viability, density, gene expression of key phenotypic, inflammatory, matrix, pain markers, and collagen accumulation.

Results: AF cells demonstrated a fibroblastic phenotype posttreatment. Moreover, transfection of SCX and MKX resulted in significant upregulation of the respective genes, as well as *SOX9*. Transfected autopsy cells demonstrated upregulation of core extracellular matrix markers; however, this was observed to a lesser effect in surgical cells. Matrix-degrading enzymes and inflammatory cytokines were downregulated, suggesting a push toward a pro-anabolic, anti-inflammatory phenotype. Similarly, pain markers were downregulated over time in autopsy cells. At the protein level, collagen content was increased in both MKX and SCX transfected cells compared to controls.

Conclusions: This exploratory study demonstrates the potential of MKX or SCX to drive reprogramming in mild to moderately degenerate AF cells from autopsy and

Connor Gantt and Ana Salazar Puerta contributed equally to this study.

This is an open access article under the terms of the [Creative Commons Attribution-NonCommercial-NoDerivs](https://creativecommons.org/licenses/by-nc-nd/4.0/) License, which permits use and distribution in any medium, provided the original work is properly cited, the use is non-commercial and no modifications or adaptations are made.

© 2023 The Authors. *JOR Spine* published by Wiley Periodicals LLC on behalf of Orthopaedic Research Society.

severely degenerate AF cells from surgical patients toward a healthy phenotype and may be a potential nonviral gene therapy for LBP.

KEYWORDS

annulus fibrosus, cell reprogramming, intervertebral disc, low back pain, nonviral transfection

1 | INTRODUCTION

Low back pain (LBP) is a leading cause of global disability with rising prevalence, and it is estimated that approximately 80% of the population suffers from LBP in their lifetime.¹⁻³ Intervertebral disc (IVD) degeneration is a significant contributor to LBP, accounting for 40% of all LBP cases.^{4,5} Yet, current clinical therapies fail to target the pathophysiology associated with IVD degeneration and rely on analgesics, physical therapy, and surgical interventions aimed at alleviating pain-related symptoms.⁶⁻⁸ This ultimately leads to temporary relief from pain but does not address the underlying causes of IVD degeneration. Thus, biological interventions that both alleviate the pain and restore healthy structure/function to the IVD are crucial.

The healthy IVD functions to provide the spine with mobility and load-bearing properties. Its structure is comprised of a gelatinous central nucleus pulposus (NP), a surrounding annulus fibrosus (AF), and superior and inferior cartilage endplates (CEP).⁹ Significantly, the outer AF plays critical roles in anchoring the IVD to adjacent vertebral bodies and resisting pressurized loads, and tensile stresses placed on the spine.^{10,11} The AF consists of an aligned matrix of collagen I and elastin network that compartmentalizes the collagen bundles, contributing to its mechanical properties in the healthy IVD.¹² The SRY-Box transcription factor 9 (SOX9), a chondrocyte marker, is also upregulated in the AF and contributes to the formation of the inner AF.¹³ Notably, transcription factors such as *Mohawk* (MKX) and *Scleraxis* (SCX) are upregulated in the healthy AF and regulate gene expression including functions associated with development, maintenance, and regeneration.^{14,15} MKX expression has been found in the outer AF and viral transfection of MKX into mesenchymal stem cells leads to regeneration of AF defects along with collagen fibril formation.^{15,16} SCX has been shown to promote tendon maturation and be a potential driver of AF regeneration as evidenced by lineage tracing in mice with herniation injuries.^{17,18}

In the diseased IVD, the structural composition of the AF becomes disorganized, leading to altered cell alignment and susceptibility to rupture.^{10,19} Degeneration leads to increased catabolic responses in the AF, including degradation of interconnecting elastin networks, upregulation of matrix degradation enzymes such as metalloproteinases (MMPs) and A disintegrin, and metalloproteinase with thrombospondin type I motifs (ADAMTs), and expression of increased inflammatory cytokines such as interleukins and tumor necrosis factor- α .²⁰⁻²³ This combination of matrix degradation and inflammation provides a permissive environment for nerve and vascular ingrowth into the AF, which has been associated with pain. Downregulation of MKX in AF cells decreases collagen expression, the expression of small leucine-rich proteoglycans such as biglycan, and other tendon/ligament-related genes (i.e., tenomodulin [TNMD],

collagen 14, SCX).¹⁵ Meanwhile, downregulation of SCX is associated with a reduction in TNMD, which is critical for the inhibition of angiogenesis and protection against IVD degeneration.^{18,24,25}

However, despite the critical role of AF in IVD function and LBP, there are limited studies regarding the AF and its targets to restore structure and function to the disc joint. SCX and MKX, as previously described, play critical roles in the AF and AF-like tissues such as tendon, and have been used to promote AF regeneration/repair and to promote an AF-like phenotype in stem cells.^{15,26-29} Yet, no studies assess the effects of MKX and SCX on mature somatic diseased AF cells and whether these factors can drive reprogramming to a healthy phenotype.

Currently, therapies targeted toward regenerating the IVD or AF include cell therapy-based approaches and the implementation of polymeric scaffolds such as fibrin–genipin, polyglycolic acid, polycaprolactone, and poly(L-lactic acid), which have shown various degrees of success.³⁰⁻³² However, there are still significant limitations with these methods, including limited cell retention and viability, and scaffold protrusion/re-herniation.³³⁻³⁶ Viral gene therapies have also been proposed to target the IVD, but risk the potential of mutagenesis and unwarranted immune responses.³⁷⁻³⁹ To overcome these limitations, nonviral transfection methods (e.g., electroporation-based approaches and nanocarriers) have been proposed as safer nonviral gene delivery systems for genetic cargo such as transcription factors.⁴⁰ Recently, studies have proposed the use of direct cell reprogramming as a promising strategy to redirect the phenotype of adult somatic cells using specific combinations of transcription factors.^{41,42} Furthermore, recent work from our group has demonstrated successful reprogramming of degenerate human NP cells toward a healthy pro-anabolic anti-catabolic phenotype mediated by the developmental transcription factors *Brachyury* or *FOXF1*. Thus, we propose applying this concept to human AF cells using MKX or SCX to promote a healthy pro-anabolic phenotype in diseased AF cells.⁴³⁻⁴⁵

Therefore, the overall goal of this proof of concept study was to assess the therapeutic effect of nonviral delivery of MKX or SCX to diseased human AF cells, to promote a healthy pro-anabolic cell phenotype. We hypothesized that transfection of MKX or SCX can increase phenotypic marker expression and collagen protein content, as well as decrease catabolic enzyme expression and secretion of inflammatory cytokines, leading to a healthier IVD.

2 | METHODS

All reagents used in this study are from Thermo Fisher Scientific or Sigma Aldrich unless otherwise stated. Percentages of reagents (%) in

TABLE 1 Autopsy and surgical sample demographics.

Sample ID	Surgical/autopsy	Level	Age	Sex	Thompson grade average
Hu13	Autopsy	L3/L4	30	Female	2.5
Hu16	Autopsy	L3/L4	19	Female	2.25
Hu19	Autopsy	L3/L4	33	Male	1.5
Hu23	Autopsy	L1/L2	42	Female	2.5
HuS-11	Surgical	L5/S1	28	Male	N/A
HuS-29	Surgical	L5/S1	70	Female	N/A
HuS-48	Surgical	L5/S1	22	Male	N/A
HuS-49	Surgical	L5/S1	64	Male	N/A

methods are % volume/volume and indicated in the manuscript as “v/v.”

2.1 | AF cell isolation from human IVDs

Autopsy lumbar spines were obtained through the Cooperative Human Tissue Network (IRB exempt) within 24 h postmortem, and IVDs were isolated, blinded, and graded according to the Thompson scale by two or more investigators (Table 1). Outer AF tissue ($N = 4$) was dissected out with ambiguous NP-AF and AF-CEP interfaces removed to avoid contamination by NP or CEP cells. AF cells were isolated using 0.03 g/mL protease (Cat: P5147-1G) in digestion media (DMEM [4.5 g/mL glucose], 1% penicillin/streptomycin [P/S, v/v], 0.5% Fungizone [v/v]) for 1 h at 37°C followed by 0.03 g/15 mL collagenase I (C2674-500MG) in digestion media for 4 h at 37°C and strained through a 70 μ m cell strainer and plated for expansion. Surgical AF tissue ($N = 4$) was obtained from patients undergoing microdissection at The Ohio State University Wexner Medical Center (IRB: 2015H0385) with cells isolated as described above. Autopsy AF cells were used as a moderately degenerate group (Thompson Grade < 3), while surgical cells were considered severely degenerate, as these cells were obtained from patients undergoing surgery for severe cases of LBP untreatable with analgesics or physical therapy.

2.2 | Cell expansion

AF cells were expanded in disc cell media (DMEM [4.5 g/mL glucose], 10% FBS [v/v], 1% P/S [v/v], 0.5% Fungizone [v/v], 50 μ g/mL ascorbic acid) in standard culture conditions and fed every 3 days until 80% confluency for downstream transfection as previously described.^{43,44} Posttransfection (passage 2), cells were plated at a cell density of $\sim 1.3 \times 10^5$ cells/cm² and fed with antibiotic-free disc cell media for 48 h before feeding with disc cell media with antibiotics for 2 weeks.

2.3 | MKX and SCX transcription factor plasmid preparation and isolation

Transformation of DH5 α competent bacterial cells was completed to generate DNA from plasmids encoding for human MKX and SCX, as

well as the control vector pCMV6-GFP (i.e., empty vector with the same backbone). All the plasmids were purchased from OriGene and are listed in Table 2. The plasmid isolation and purification were carried out using the ZymoPURE™ II Plasmid Miniprep Kit (Zymo Research, D4201), following the procedure described by the manufacturer. DNA concentration and quality were measured by spectrophotometry using a Nanodrop 2000c Spectrophotometer.

2.4 | Nonviral MKX and SCX transfection

Nonviral cell transfection of human AF cells ($N = 4$, pooled) from surgical and autopsy samples was performed using a Neon transfection system. Once the cells (passage 1) reached $\sim 80\%$ confluency, they were detached and resuspended at a final concentration of 1.0×10^4 cells/mL in electrolytic buffer. Briefly, the system implements an electric field (1 pulse of 1425 V for 30 ms) which transiently porates the cell membrane and facilitates plasmid delivery into the cells as shown in Figure 1. Cells were transfected with plasmids encoding for MKX and SCX at two different concentrations (0.05 and 0.1 μ g/ μ L; $N = 6$ transfection replicates). The SHAM vector pCMV6-GFP was used as control at the same concentrations (0.05 and 0.10 μ g/ μ L; $N = 4$ transfection replicates).

2.5 | Dependent variables

Cells were collected up to 2 weeks after transfection and morphology (48 h), gene expression (48 h, 7 days, 14 days), and collagen content (7 and 14 days) were characterized.

2.5.1 | Cell viability, density, and morphology

To measure cell viability, cultured cells were washed with $1 \times$ PBS twice and stained with Calcein (1:1000, Cat# C1430) for 10 min. The cells were then washed with $1 \times$ PBS twice and fixed in 10% neutral buffered formalin for 10 min at room temperature, washed with PBS again, and followed by 0.1% Triton X-100 in PBS for 20 min to permeate the cells. After permeation, the samples were washed with PBS before adding Phalloidin (1:400, Cat# R415) to visualize actin and Hoechst

TABLE 2 Plasmids used in the study.

Plasmid	Species	CAT #	Size (kb)	Antibiotic resistance	Vector
pCMV6 (SHAM)	NA	PS100010	6.6	Ampicillin (100 µg/mL)	pCMV6-AC-GFP
Mohawk homeobox	Human	RG206923	7.6	Ampicillin (100 µg/mL)	pCMV6-AC-GFP
Scleraxis (SCXA)	Human	RG224305	7.2	Ampicillin (100 µg/mL)	pCMV6-AC-GFP

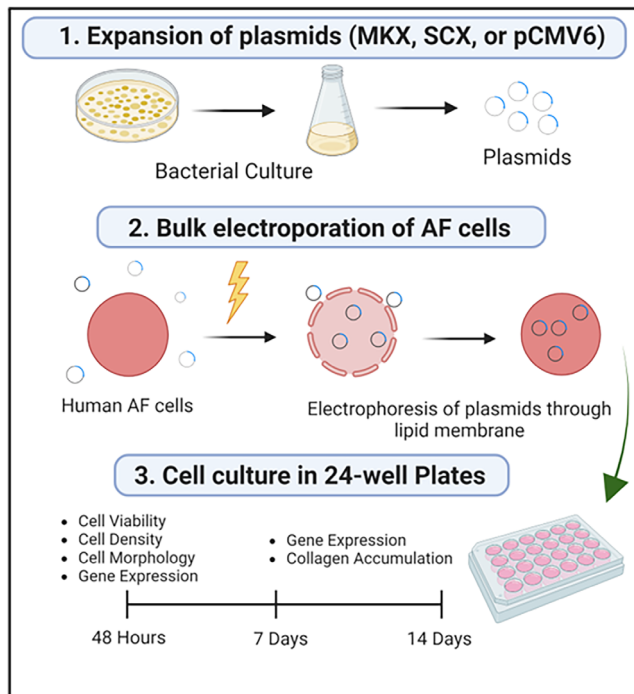


FIGURE 1 Schematic of the research design with (1) expansion of plasmids (Mohawk [MKX], Scleraxis [SCX], or pCMV6) via bacterial culture followed by (2) nonviral bulk transfection of 0.05 or 0.10 µg/µL doses of MKX, SCX, or the respective pCMV6 plasmids and (3) seeding for downstream assessments of cell viability, cell density, morphology, gene expression, and collagen accumulation over 14 days.

(1:2000, Cat# H1399) for nuclei, and let to incubate at room temperature for 30 min before imaging at 20× and 10× using a fluorescent Nikon inverted Ti-Eclipse microscope. Images were then quantified for viability as the number of viable cells (Calcein) over the total number of cells (Hoechst), and for density as the number of cells (Hoechst) per image field. Cellular morphology was assessed via qualitative observations to account for over confluent regions in the samples.

2.5.2 | Gene expression

mRNA from the samples was isolated using the Trizol Plus RNA Purification Kit (Cat# 12183555). Briefly, cells were digested in 1 mL of Trizol and 0.2 mL of chloroform was added for phase separation. Seventy percent ethanol (v/v) was added to the clear phase at a 1:1 ratio and binding, washing, and elution of RNA was completed per manufacture protocol. cDNA was synthesized with Maxima H Minus

TABLE 3 Taqman gene expression assay information.

Primer	TaqMan assay ID
Mohawk	Hs00543190_m1
Scleraxis	Hs03054634_g1
Elastin	Hs00355783_m1
IL-1β	Hs00174097_m1
IL-6	Hs00174131_m1
MMP1	Hs00899658_m1
MMP2	Hs01548727_m1
NGF	Hs00171458_m1
BDNF	Hs03805848_m1
Biglycan	Hs00959143_m1
ADAMTS6	Hs01552731_m1
SOX9	Hs00165814_m1
18S	4333760F

Mastermix (Cat: M1662) per manufacture protocol. RT-qPCR was run on 384 well plates as previously described with the primers listed in Table 3.^{43,44} Gene expression data were analyzed via the comparative $2^{-\Delta\Delta Ct}$ method normalized to 18S and presented as fold change with respect to SHAM.⁴⁶

2.5.3 | Collagen content

Total collagen content was assessed using the soluble Sircol assay (BioVendor, Cat#S1000) per manufacturer's protocol. Briefly, cells were collected from each sample using 0.25% trypsin and pelleted with media aspirated. Two hundred microliters of 0.1 mg/mL Pepsin in 0.5 M acetic acid were then added to each pellet and placed at 4°C with mechanical agitation to let digest overnight. 100 µL of the digest was transferred to a new tube with 1 mL of Sircol Dye reagent added and mechanically agitated for 30 min to form a collagen dye complex precipitate. Tubes were then spun down at 13 000×g for 10 min and drained to remove residual unbound dye. Before adding alkali reagents, 750 µL of ice-cold acid salt wash reagent was layered onto each pellet for washing. The samples were measured using a spectrometer for overall collagen content (no specificity in collagen type).

2.5.4 | Statistical analysis

All data were analyzed using Excel with statistical analysis and graph construction completed with GraphPad Prism Software. For gene

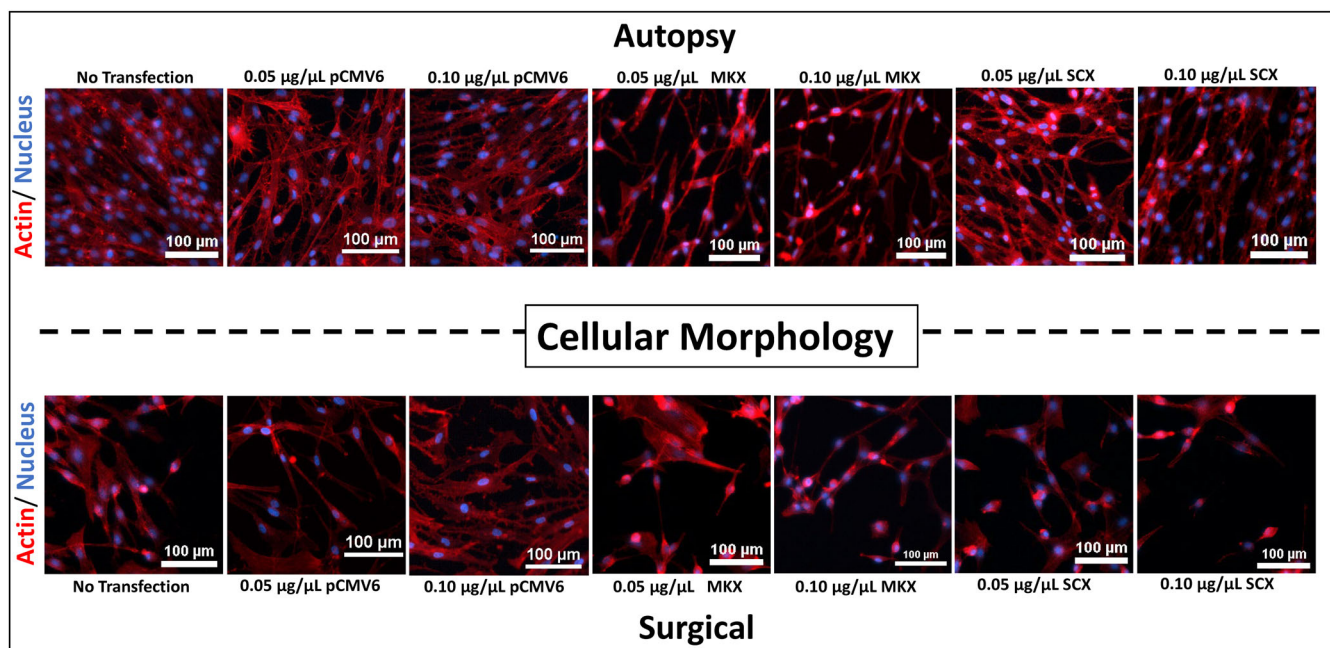


FIGURE 2 Cellular morphology at 48 h posttransfection as indicated by phalloidin staining (red) of cellular actin with Hoechst nuclei staining (blue). The top row represents autopsy cells while the bottom row represents surgical cells for nontransfected control, 0.05 µg/µL SHAM, 0.10 µg/µL SHAM, 0.05 µg/µL MKX, 0.10 µg/µL MKX, 0.05 µg/µL SCX, and 0.10 µg/µL SCX (scale bar = 100 microns).

expression and cell density/viability data, significant differences between each group over time were assessed using a Kruskal–Wallis test with $\alpha = 0.05$ where a p -value of $p < 0.05$ was considered to be statistically significant. A Kruskal–Wallis test was used as the data not being normally distributed after confirmation with a Shapiro–Wilks test. The effect of time and treatment on collagen accumulation was assessed using a multilinear model accounting for the small sample size and nonparametric data with effects and interactions of time (48 h, 7 days, 14 days), treatments, and interactions of time \times treatment. Data throughout the manuscript are represented as mean and standard deviation (SD) as described in each figure legend. All figures include $N = 4$ for SHAM groups and $N = 6$ for MKX and SCX transfected groups, respectively with error bars representing SD.

3 | RESULTS

3.1 | Cell viability, density, and morphology

Qualitative assessment of cell morphology via phalloidin staining of cellular actin exhibited elongated fibroblast-like morphology in all groups including nontransfected control, SHAM (0.05, 1.0 µg/µL), and MKX and SCX transfected groups (Figure 2). Cell viability at 48 h, quantified via live cells over the total number of cells, showed a high percentage of viable cells with no significant differences between experimental groups in both autopsy (average = 89%) and surgical (average = 88%) cells (Figure 3). Cell density quantified via the total number of cells within the imaged field was significantly lower for surgical cells transfected with 0.10 µg/µL MKX (39.8 cells/field,

$p = 0.0225$) and 0.10 µg/µL SCX (35.5 cells/field, $p = 0.0094$) compared to those transfected with 0.05 µg/µL SHAM (82.0 cells/field). In addition, surgical cells transfected with 0.10 µg/µL SCX had lower cell density compared to those transfected with a low dose (0.05 µg/µL) of MKX (70.0 cells/field, $p = 0.0264$) and SCX (75.3 cells/field, $p = 0.0195$). Autopsy cells transfected with a high dose (0.10 µg/µL) of SCX had higher cell density compared to those transfected with a low dose (0.05 µg/µL) of SHAM ($p = 0.0170$; Figure 3).

3.2 | Gene expression

Gene expression data are presented as a fold change for each group with respect to their respective SHAM dose at each time point.

3.2.1 | Transcription factors

MKX gene expression was significantly upregulated at 48 h for both doses of MKX, with a fold change of 9.6 and 19.2 for autopsy cells and a fold change of 41.4 and 119 for surgical cells transfected with 0.05 µg/µL and 0.10 µg/µL MKX, respectively, compared to SHAM and SCX transfection (Figure 4A, $p < 0.05$). MKX gene expression was significantly upregulated at 7 days, with a fold change of 2.6 in autopsy and 4.2 in surgical cells with 0.10 µg/µL of MKX compared to 0.05 µg/µL of MKX or SCX ($p < 0.05$). At 14 days, no differences were observed in MKX expression. Meanwhile, SCX gene expression was significantly upregulated in both autopsy and surgical cells with SCX transfection at both doses; fold changes of 175 and 691 for

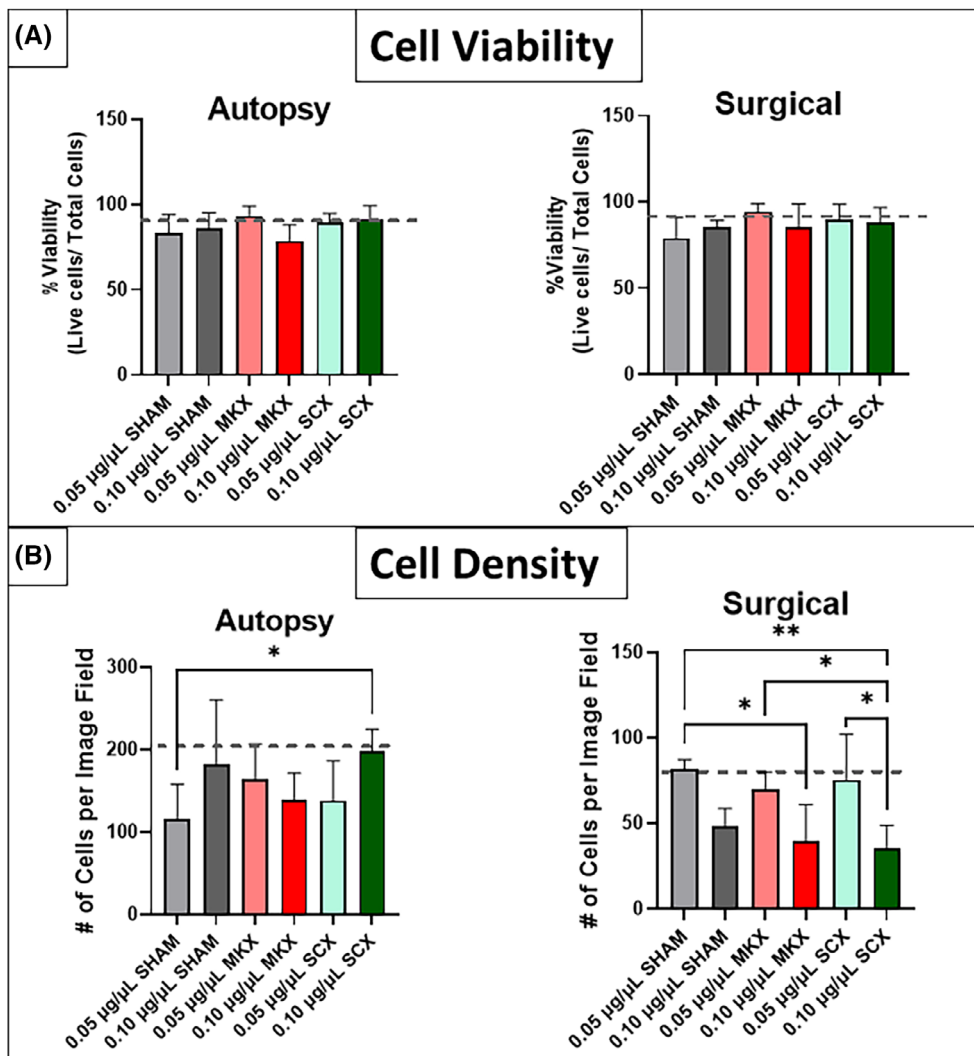


FIGURE 3 (A) Cell viability of autopsy and surgical cells posttransfection of Mohawk (MKX) and Scleraxis (SCX), respectively quantified by the number of live cells over total cells. (B) The cell density of autopsy and surgical cell posttransfection with MKX and SCX, respectively quantified as the number of cells per imaged field. The dashed line represents nontransfected control thresholds. * $p < 0.05$; ** $p < 0.01$.

autopsy and 518 and 3529 for surgical cells were noted compared to SHAM and transfection with MKX at 48 h (Figure 4B, $p < 0.01$). At 7 days, SCX transfection with 0.05 µg/µL significantly increased SCX expression compared to SHAM and MKX for autopsy cells with a fold change of 45.9 and both doses of SCX transfection increased SCX expression with fold changes of 42.3 and 183 in surgical cells compared to SHAM and MKX ($p < 0.05$). At 14 days, there was a significant increase in SCX expression at 0.05 µg/µL SCX with a fold change of 16.7 compared to SHAM for autopsy cells ($p = 0.0319$) and significant increases in SCX expression at both doses of SCX with fold changes of 9.1 and 22.7 in surgical cells compared to SHAM and MKX treatment ($p < 0.05$). Moreover, SOX9 was significantly upregulated with a fold change of 269 at a dose of 0.10 µg/µL MKX, a fold change of 393 at a dose of 0.05 µg/µL SCX, and a fold change of 159 for the 0.10 µg/µL SCX group at 14 days in autopsy cells compared to SHAM groups (Figure 4C, $p < 0.05$). In surgical cells, MKX and SCX transfection at all doses and time points significantly upregulated SOX9 expression compared to SHAM groups with fold changes of 1698, 1295, 284, and 566 for 0.05 µg/µL MKX, 0.10 µg/µL MKX, 0.05 µg/µL SCX, and 0.10 µg/µL SCX

respectively at 48 h. Fold changes at 7 and 14 days were 1000, 494, 895, 433 and 317, 233, 839, and 202, respectively.

3.2.2 | ECM phenotypic markers

In autopsy cells, elastin gene expression was significantly upregulated in 0.05 µg/µL SCX transfected groups at 48 h with a fold change of 3.29 and both doses of SCX at 14 days with a fold change of 4.7 and 2.9 respectively, compared to SHAM or MKX transfection groups (Figure 5A, $p < 0.05$). Elastin was also upregulated in 0.05 µg/µL MKX transfected groups at 7 days with a fold change of 4.3 compared to SHAM or SCX transfection groups (Figure 5A, $p = 0.0036$). However, in surgical cells, elastin was significantly downregulated in 0.05 µg/µL MKX, 0.10 µg/µL MKX, and 0.05 µg/µL SCX groups with fold changes of -4.61 , -3.31 , and -7.06 , respectively, at 7 days. At 14 days, 0.05 µg/µL doses of MKX and SCX had downregulated elastin with fold changes -11.3 and 4.37 compared to SHAM and higher doses ($p < 0.05$). Biglycan expression was significantly upregulated in 0.10 µg/µL MKX, 0.05 µg/µL SCX, and 0.10 µg/µL SCX groups with

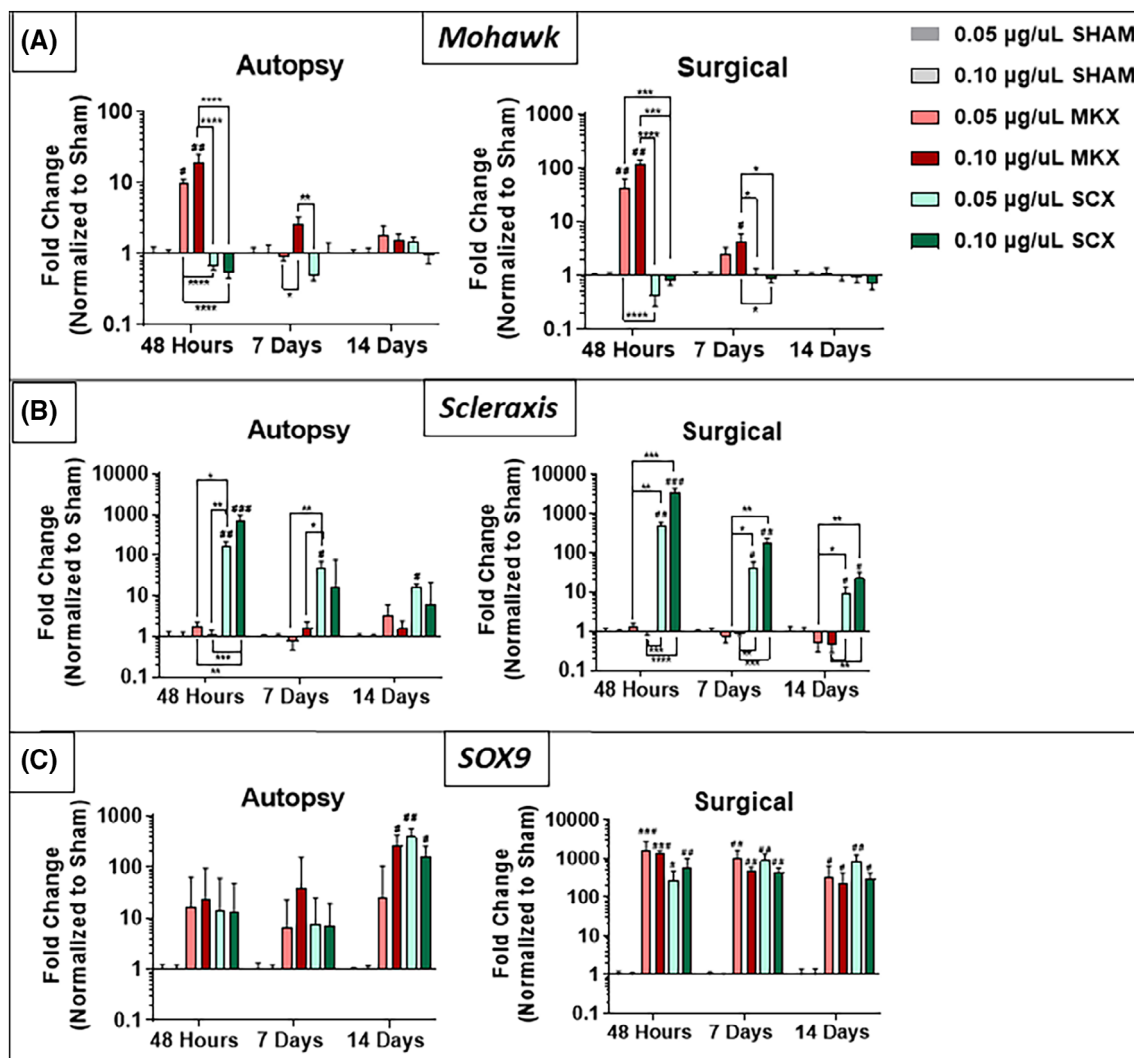


FIGURE 4 Transcription factor gene expression: (A) Mohawk (*MKX*), (B) Scleraxis (*SCX*), and (C) *SOX9* gene expression normalized to respective SHAM groups for *SCX* and *MKX* transfected cells at 48 h, 7 days, and 14 days, respectively, for (right) autopsy and (left) surgical cells. #*p* < 0.05 compared to SHAM (*p*CMV6); ##*p* < 0.01; ###*p* < 0.001; **p* < 0.05; ***p* < 0.01; ****p* < 0.001; *****p* < 0.0001.

fold changes 7.74, 7.67, and 4.97, respectively, at 14 days in autopsy cells while downregulated in 0.05 µg/µL *SCX* with a fold change of -9.63 at 48 h in surgical cells compared to SHAM groups (Figure 5B, *p* < 0.05).

3.2.3 | Inflammatory cytokines

In autopsy cells, interleukin 1 beta (*IL-1β*) was downregulated in all *MKX* doses and 0.05 µg/µL *SCX* transfected groups at 48 h compared to SHAM groups with fold changes of -3.57 , -2.51 , and -3.67 , respectively. No significant differences were observed at later time points (Figure 6A, *p* < 0.05). In surgical cells, no differences were observed between *MKX* and *SCX* compared to SHAM at 48 h and 7 days with downregulation of *IL-1β* in 0.05 µg/µL *MKX* transfected groups at 14 days with a fold change of -3.08 . Differences in interleukin 6 (*IL-6*) gene expression were observed at 14 days between

MKX and *SCX* transfected groups in autopsy samples, but no significant differences were found compared to SHAM. In surgical cells, *IL-6* was downregulated at 7 days in 0.05 µg/µL *MKX* and *SCX* groups with fold changes of -8.96 and -5.29 and at 14 days with fold changes of -9.90 and -7.55 relative to SHAM. Surgical cells treated with 0.10 µg/µL *MKX* were also downregulated at 14 days with a fold change of -4.23 (Figure 6B, *p* < 0.05).

3.2.4 | Matrix-degrading enzymes

No significant differences in *MMP1* and *MMP2* were observed in autopsy cells at 48 h and 7 days compared to SHAM groups apart from increased *MMP1* in 0.05 µg/µL *SCX* groups with a fold change of 2.79 at 14 days (Figure 7A,B). In surgical cells however, *MMP1* was downregulated at 7 days in 0.05 µg/µL *SCX* transfected groups with a fold change of -4.25 and downregulated in both 0.05 µg/µL *MKX*

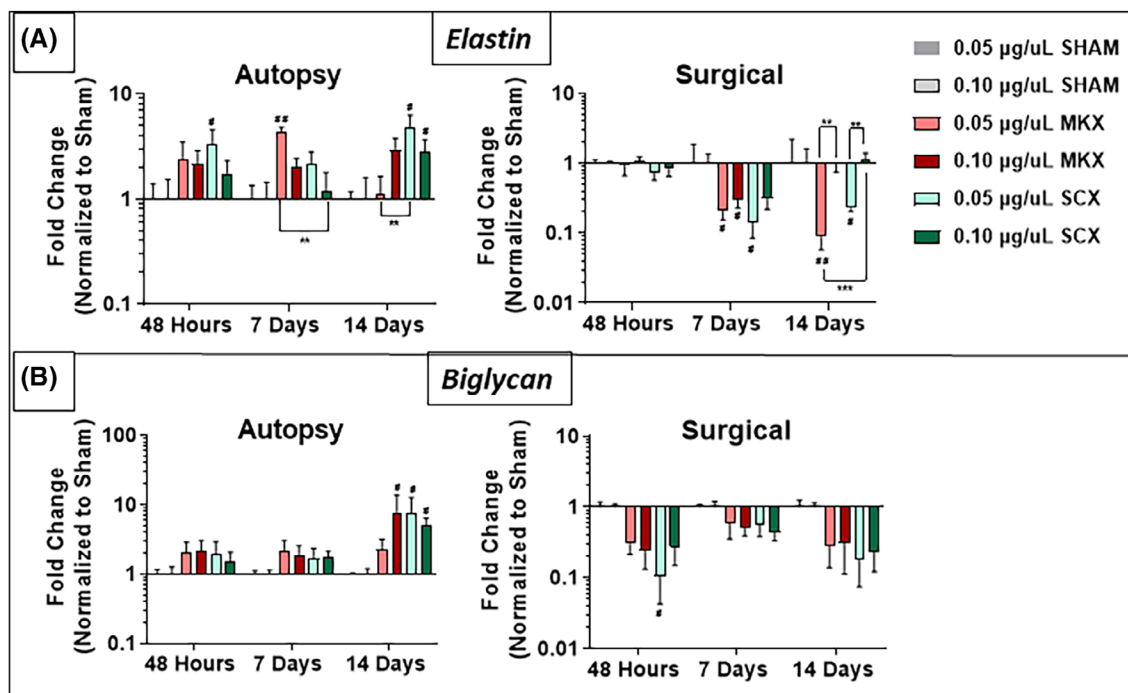


FIGURE 5 Extracellular matrix phenotypic markers: (A) elastin and (B) biglycan, gene expression normalized to respective SHAM groups for Scleraxis (SCX) and Mohawk (MKX) transfected cells at 48 h, 7 days, and 14 days respectively for (right) autopsy and (left) surgical cells. # $p < 0.05$ compared to SHAM (pCMV6); ## $p < 0.01$; * $p < 0.05$; ** $p < 0.01$; *** $p < 0.001$.

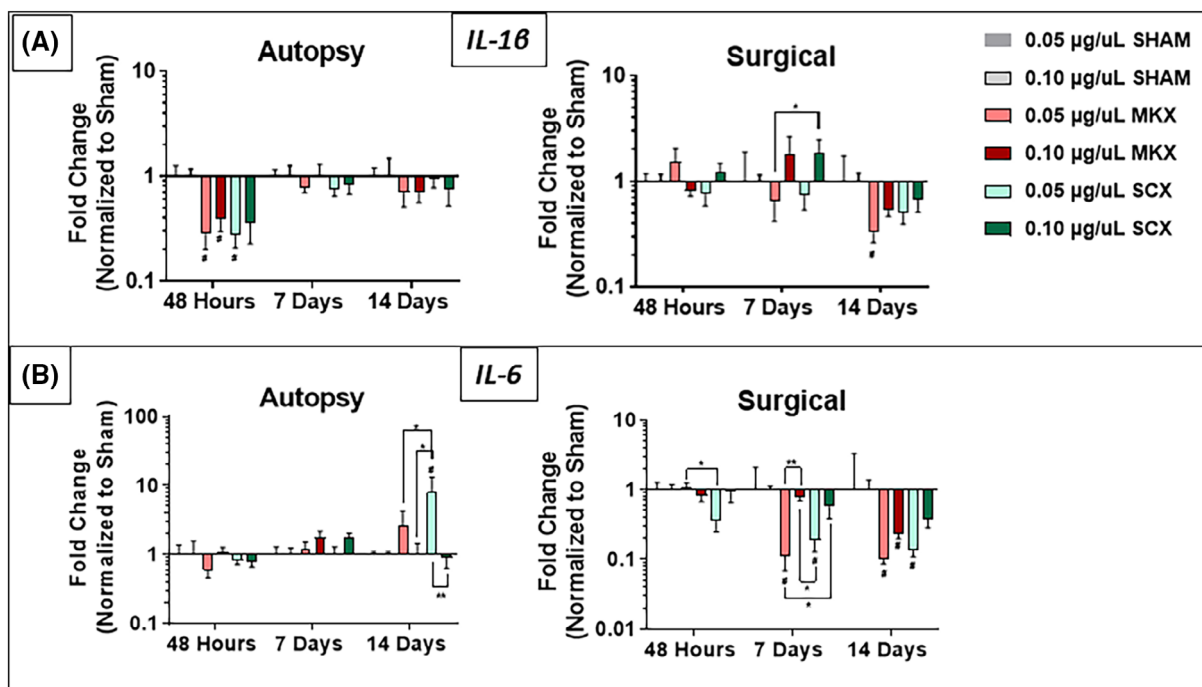


FIGURE 6 Inflammatory cytokines: *IL-1 β* and *IL-6* gene expression normalized to respective SHAM groups for Scleraxis (SCX) and Mohawk (MKX) transfected cells at 48 h, 7 days, and 14 days, respectively, for (right) autopsy and (left) surgical cells. # $p < 0.05$ compared to SHAM (pCMV6); * $p < 0.05$; ** $p < 0.01$.

and SCX groups with fold changes of -13.5 and -8.40 at 14 days compared to SHAM or higher dose MKX or SCX transfection groups ($p < 0.05$). Similarly, *MMP2* was significantly downregulated in both

MKX groups with fold changes of -2.72 , -3.03 and in the $0.10 \mu\text{g}/\mu\text{L}$ SCX group with a fold change of -2.41 at 14 days compared to SHAM ($p < 0.05$). For *ADAMTS6* expression in autopsy cells, no

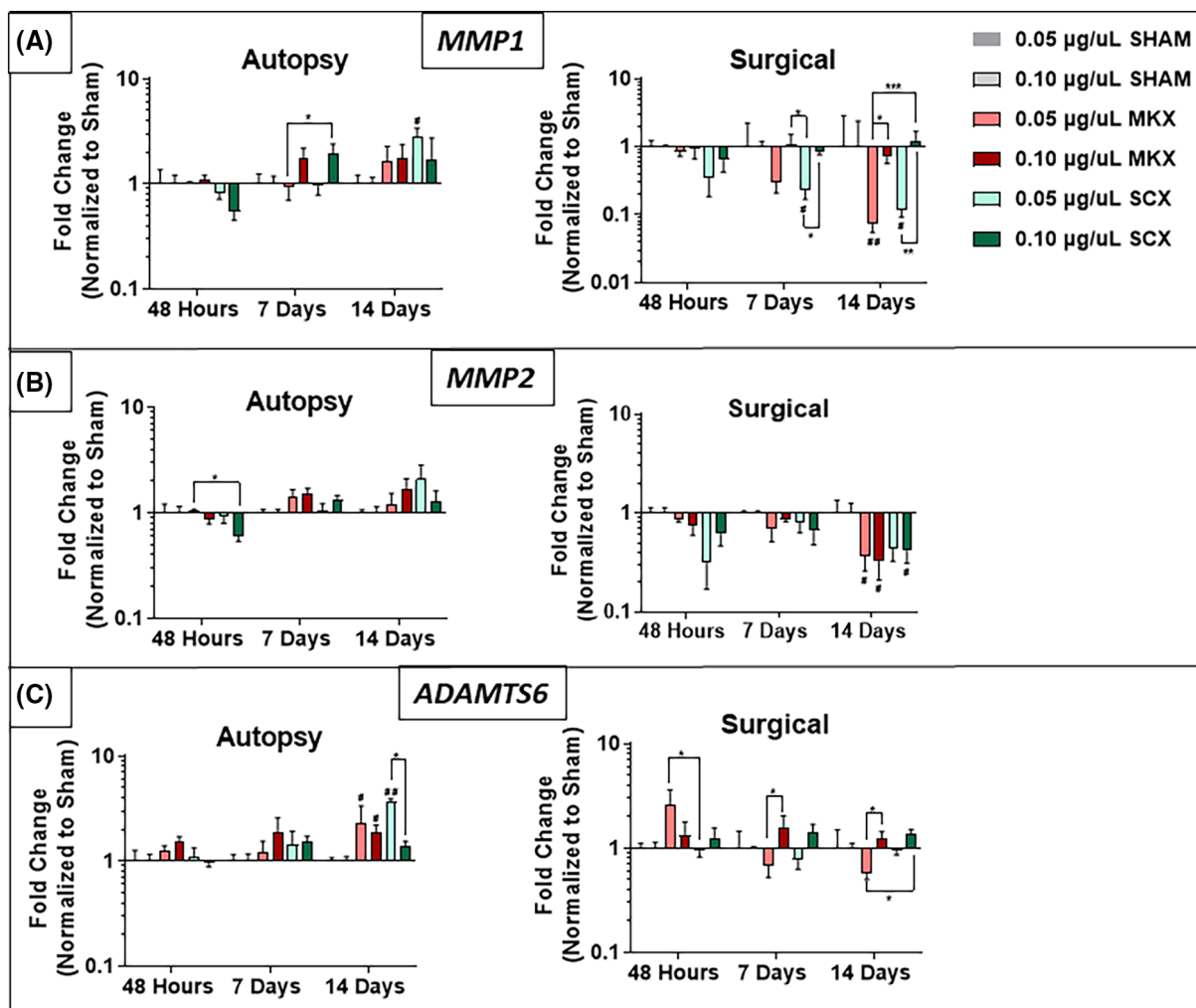


FIGURE 7 Matrix degradation: (A) *MMP1*, (B) *MMP2*, and (C) *ADAMTS6* gene expression normalized to respective SHAM groups for Scleraxis (SCX) and Mohawk (MKX) transfected cells at 48 h, 7 days, and 14 days, respectively, for (right) autopsy and (left) surgical cells. # $p < 0.05$ compared to SHAM (pCMV6); ## $p < 0.01$; * $p < 0.05$; ** $p < 0.01$; *** $p < 0.001$.

significant differences were observed at 48 h or 7 days. However, increased expression in MKX transfected groups was observed at 14 days with fold changes of 2.213, and 1.89, and in 0.05 $\mu\text{g}/\mu\text{L}$ SCX groups with a fold change of 3.65 compared to SHAM or high dose of SCX. In surgical cells, no differences were observed with transfection compared to SHAM controls (Figure 7C).

3.2.5 | Pain markers

In autopsy cells, no difference in nerve growth factor (NGF) was observed at earlier time points with upregulation at 14 days in 0.05 $\mu\text{g}/\mu\text{L}$ SCX transfected groups compared to SHAM with a fold change of 4.41 (Figure 8A, $p = 0.0231$). No significant differences in NGF were observed in surgical cells compared to SHAM. Brain-derived neurotrophic factor (BDNF) was upregulated in high-dose MKX transfected groups at 7 days with a fold change of 2.70 with no other significant differences in autopsy cells ($p = 0.0331$). In surgical cells, BDNF was downregulated in both 0.05 $\mu\text{g}/\mu\text{L}$ MKX and

SCX transfection groups with fold changes of -3.05 and -3.44 , respectively, compared to SHAM and high dose MKX group ($p < 0.05$).

3.3 | Collagen content

Cellular collagen protein content as measured by the Sircol assay at 7 and 14 days showed significant increases in collagen across all transfection groups compared to SHAM in both autopsy and surgical cells, while SHAM transfection resulted in lower than 2 $\mu\text{g}/\text{well}$ of collagen accumulation (Figure 9). In detail, autopsy cells at 7 days averaged 5.25 $\mu\text{g}/\text{well}$ in the low dose (0.05 $\mu\text{g}/\mu\text{L}$) MKX group and 4.32 $\mu\text{g}/\text{well}$ collagen in the high dose (0.05 $\mu\text{g}/\mu\text{L}$) MKX group while SCX groups averaged 5.43 $\mu\text{g}/\text{well}$ in the low dose group and 5.37 $\mu\text{g}/\text{well}$ in the high dose group ($p < 0.001$). At 14 days, MKX groups averaged 7.025 $\mu\text{g}/\text{well}$ at the low dose and 5.85 $\mu\text{g}/\text{well}$ at the high dose, while SCX groups averaged 6.15 and 7.10 $\mu\text{g}/\text{well}$ respectively ($p < 0.0001$). Interestingly, transfected groups did not

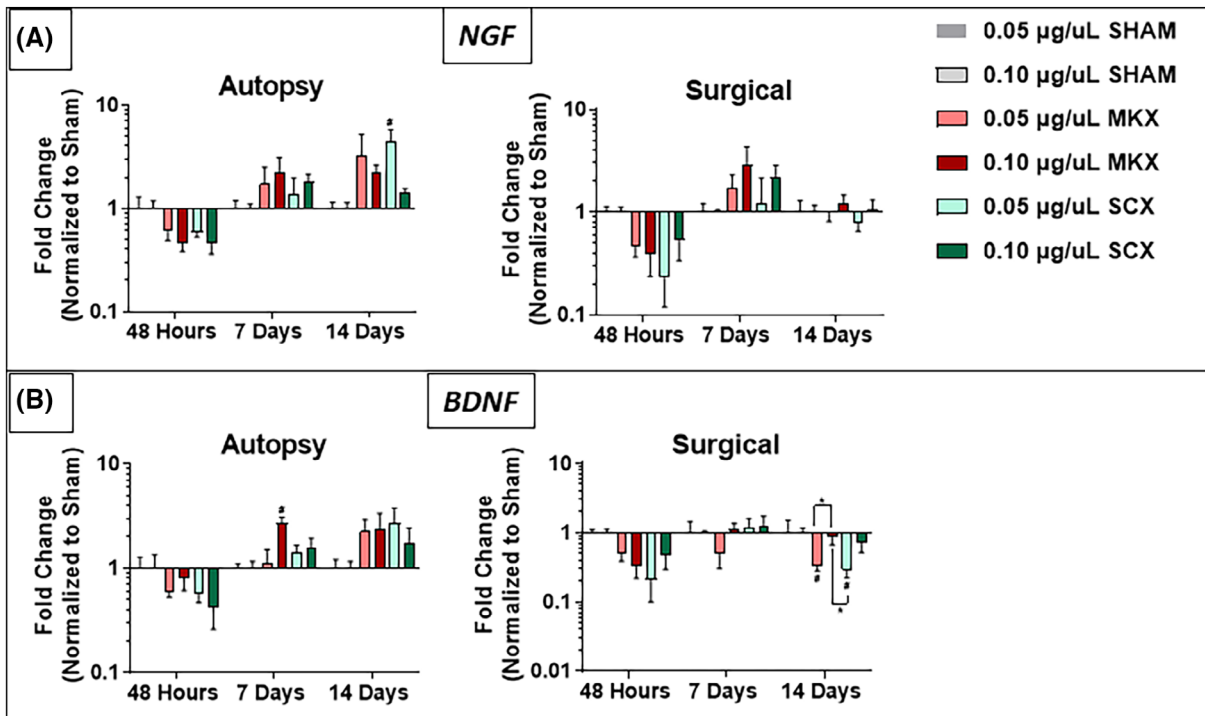


FIGURE 8 Pain markers: (A) nerve growth factor (NGF) and (B) brain-derived neurotrophic factor (BDNF) gene expression normalized to respective SHAM controls for Scleraxis (SCX) and Mohawk (MKX) transfected cells at 48 h, 7 days, and 14 days, respectively, for (right) autopsy and (left) surgical cells. #*p* < 0.05 compared to SHAM (pCMV6), **p* < 0.05.

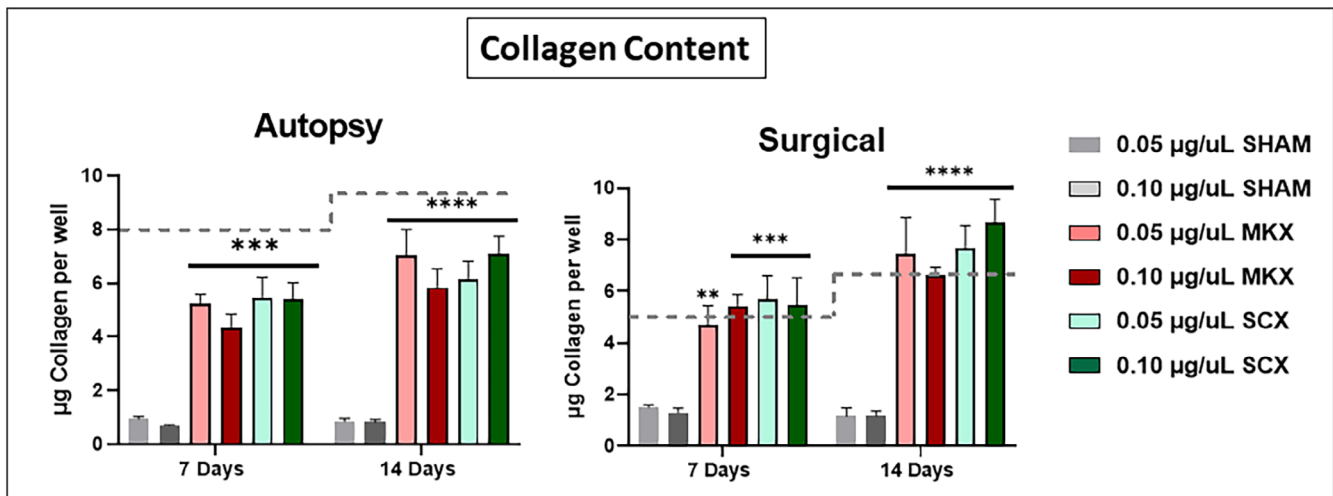


FIGURE 9 Collagen content of SHAM (pCMV6), Mohawk (MKX), and Scleraxis (SCX) transfected autopsy and surgical cells at 7 and 14 days posttransfection, respectively. Horizontal bars indicate statistical significance compared to SHAM (*****p* < 0.0001; ****p* < 0.001). Dashed lines indicate nontransfected control cells.

accumulate levels of collagen beyond the threshold of nontransfected control cells indicated by the dashed line in Figure 9. Surgical cells at 7 days averaged 4.68 µg/well (*p* < 0.01) in low dose and 5.43 µg/well in high dose MKX transfection groups while SCX averaged 5.68 and 5.46 µg/well respectively (*p* < 0.001). At 14 days, MKX transfected groups averaged 7.47 and 6.10 µg/well at low and high doses, while SCX groups averaged 7.68 and 8.65 µg/well, respectively (*p* < 0.0001). Also, in surgical samples, transfected groups

accumulated more collagen than nontransfected severely degenerate surgical control cells.

4 | DISCUSSION

This exploratory study used developmental transcription factors MKX and SCX to reprogram degenerate human AF cells isolated from both

autopsy specimens and surgical specimens from patients with LBP to a healthy phenotype as demonstrated by significant changes in cellular markers such as key transcription factors including pro-anabolic, catabolic, and inflammatory-pain-related factors that we will discuss in the following paragraphs. As the AF is currently understudied with respect to IVD degeneration, this study reveals the potential of treatment with *MKX* and *SCX* as a nonviral gene therapy for degenerate AF cells to restore proper structure/function to the IVD.

4.1 | Effect of *MKX* or *SCX* transfection on cell morphology, viability, and density

All the cells used for this study exhibited a fibroblast-like morphology in nontransfected control, SHAM, and experimental groups, which aligns with literature reports about AF morphology. Notably, increases in cell processes/branches can be seen in *MKX* and *SCX* transfected groups (Figure 2), which resemble the phenotype of outer AF cells.⁴⁷ The lack of differences in cell viability at 48 h suggests that there are no significant changes in cell survivability post-seeding. However, the decreased cell density observed for surgical cells can be linked to the degenerative nature/state of the surgical samples derived from patients with advanced IVD degeneration. Moreover, these cells were more susceptible to the standard electroporation-based transfection method used in this study. This type of transient transfection could additionally explain some parts of the results observed in this study.

4.2 | *SCX* and *MKX* upregulate key transcription factors

The significant upregulation of *MKX* and *SCX* gene expression in our respective *MKX* and *SCX* transfected groups (Figure 4) demonstrates successful nonviral transfection of these transcripts into both autopsy and surgical human AF cells. While *SCX* was significantly upregulated over time, *MKX* expression was not sustained over time. This could indicate a transient effect of transfection via bulk electroporation (BEP), however, the effects of the transfection were observed from other genes. Interestingly, no significant differences in *MKX* or *SKX* expression were noted between the two different doses tested, suggesting limited dose-dependent effects. An alternative and minimally invasive mechanism of delivery may be warranted, which could provide better outcomes compared to BEP. Interestingly, *SOX9*, a chondrocyte-specific transcription factor was highly upregulated post-*MKX* and *SCX* treatment, suggesting *MKX* and *SCX* may promote regulation of *SOX9* which conflicts with studies suggesting that *MKX* functions as a repressor of *SOX9*.¹⁵ *SOX9* has also been shown to promote inner AF collagen and proteoglycan synthesis after adenoviral delivery^{13,48} and based on our findings may also function downstream of *MKX* and *SCX* for the repair of outer AF cells. Upon further investigation, we also assessed gene expression of key AF phenotypic markers such as cluster of differentiation 146 (CD146/MCAM), Fibulin (FBLN), and integrin binding sialoprotein (IBSP), which would

differentiate these AF cells from their NP counterparts (Figure S1).⁴⁹⁻⁵¹ CD146 is a cell adhesion molecule found in the outer AF and highly upregulated in the AF compared to NP while FBLN and IBSP were found to be significantly expressed in AF tissue and may serve as AF specific/NP negative marker. Some significant differences were observed in *MKX* or *SCX* transfected groups compared to SHAM, especially for the surgical group; however, these were either dose-dependent or temporal. This may be associated with the nature of BEP and further studies using minimally invasive gene delivery approaches along with deep transcriptome characterization such as RNAseq may further elucidate the reprogramming potential of *MKX* and *SCX* to drive an AF-specific phenotype.

4.3 | Regulation of extracellular matrix and homeostasis

In terms of evaluating the anabolic effect of our reprogramming strategy, we investigated the expression of key ECM-related genes involved in AF homeostasis. Elastin is an important protein found in the network of the interlamellar matrix of the AF that aids in the IVDs ability to withstand mechanical loading. Thus, the upregulation of elastin in AF cells from autopsy samples transfected with *MKX* and *SCX* may support their role in upregulation of elastin in mildly degenerate samples, which contributes to a healthy AF environment. Interestingly, elastin was downregulated in surgical samples, which could be due to the severely degenerate nature of these cells from patients experiencing chronic LBP. However, there is conflicting evidence as to whether elastin content increases with aging or IVD degeneration.⁵² The same trends were observed for biglycan, with upregulation for autopsy cells transfected with a high dose (0.10 µg/µL) of *MKX* and a low dose (0.05 µg/µL) of *SCX* at 14 days. On the other hand, no significant differences in biglycan expression were observed for surgical cells. Biglycan plays a role in maintaining homeostatic processes in the AF and loss of expression has been noted in IVD degeneration.⁵³ However, studies have also shown upregulation of biglycan in diseased IVDs.⁵⁴ Thus, the results from elastin and biglycan gene expression suggest a pro-anabolic drive of mildly degenerate AF cells after *MKX* and *SCX* transfection but may require further optimization for more degenerated AF cells.

To investigate the anti-catabolic effects of *MKX* and *SCX* transfection, we evaluated the gene expression of key matrix degradative enzymes in the AF, including *MMP1*, *MMP2*, and *ADAMTS6*, which are involved in the breakdown of the AF ECM, causing a progressive shift from anabolic to catabolic processes.²⁰ Downregulation of *MMP1* and *MMP2* in severely degenerate surgical samples suggests anti-catabolic rescue after transfection with *MKX* and *SCX* to push pro-anabolic processes on diseased AF cells.

On the protein level, *SCX* and *MKX* transfection promoted significantly higher accumulation of collagen, a critical AF ECM component, in comparison to SHAM transfected cells, where less than 2 µg of collagen was accumulated. The large increase in collagen synthesis/accumulation suggests that the AF cells are reverting to a healthy

native state post-treatment which may have considerable impact in the severely degenerate IVD, where the accumulation of collagen exceeds nontransfected controls. In conjunction with key ECM and matrix degradation markers, *MKX* and *SCX* transfection may guide diseased AF cells toward a pro-anabolic phenotype and maintain cellular homeostasis.

4.4 | Effects of *MKX* and *SCX* on downstream inflammatory markers

Inflammatory cytokines, such as *IL-1 β* and *IL-6*, have been observed in the degenerate AF and can also upregulate *MMPs* and *ADAMTSs*.^{20,21,55,56} *IL-1 β* expression was downregulated at early time points in autopsy samples and consistently downregulated in surgical samples over time, which suggests decreased inflammation in surgical cells. Interestingly, this correlates with previous findings where *FOXF1*⁴⁴ and *Brachyury*⁴³ were nonvirally transfected into degenerate NP cells, with greater downregulation of *IL-1 β* and *IL-6* observed compared to autopsy cells.

4.5 | Effect of *MKX* and *SCX* on in vitro pain predictors

NGF and *BDNF* were used as pain predictors in this in vitro study. These factors also play a role in the potentiation of IVD degeneration and nerve ingrowth.^{57,58} While downregulation of *NGF* and *BDNF* was observed in surgical samples, they were upregulated over time in autopsy samples. This suggests potential regulation of pain associated with *MKX* and *SCX*; however, the delivery method warrants optimization as pain is a major predictive outcome measure of successful discogenic therapies.

4.6 | Nonviral transfection and AF therapies

Previous biologic therapies for AF include the use of growth factors such as bone morphogenic protein (*BMP-1*, *BMP-2*, and *BMP-3*), Tumor growth factor Beta, and growth differentiation factor 5,^{59–63} which have shown success in increasing collagen content and re-establishing homeostasis with the reduction of *MMPs*. However, direct delivery of growth factors is limited by their half-life and may not be suitable as a long-term therapy for IVD degeneration and back pain. Thus, gene therapies may provide a long-term solution. Currently, most studies involving genetic therapies for the IVD are conducted via the use of adeno-associated virus, mainly due to their high transfection efficiency. However, their implementation can be clinically limited by their mutagenic and immunogenic potential.⁶⁴ Thus, nonviral delivery is advantageous to overcome these limitations. Moreover, the delivery of transcription factors to drive reprogramming of AF cells toward a healthy phenotype is an innovative and viable approach as we have demonstrated here. In addition, previous

studies have looked at the therapeutic potential of delivering AF-like cells derived from human iPSCs or the use of stem cells, which also have limitations such as low cell survivability due to the harsh IVD environment.^{16,65} Therefore, this study proposes the use of nonviral delivery of the critical developmental transcription factors *SCX* and *MKX*, to drive reprogramming of native cells, already adapted to the IVD environment, toward a healthy phenotype. While *SCX* and *MKX* both have great potential, the results of this drive further reprogramming along with further optimized delivery methods.

4.7 | Potential limitations and future directions

It is important to note the limitations of this study which include the use of BEP, pooling of multiple human samples for experimental replicates to limit variability, and the use of standard monolayer well plates for in vitro culture. BEP, while serving as a good method for validating downstream effects of transfected factors, may cause necrosis, cellular dysfunction, and potential senescence due to the use of high non-localized electric fields, which disrupts the lipid bilayer as discussed in previous studies.^{43,44,66,67} Thus, further studies improving the delivery mechanism of these transcription factors are warranted, such as engineered extracellular vesicles (EVs), which harbor many advantages including nonimmunogenic characteristics, reduced potential of mutagenesis, and tunability for multiple applications.^{41,42,68} In addition, human AF samples were pooled for our proof-of-concept study, and transfection replicates were examined to reduce variability and explore the effects of all samples within the pool. However, studies^{69,70} have shown demographical differences such as sex and age in response to therapeutic approaches, and thus future studies will need to incorporate multiple demographical groups (e.g., elderly, young, male, and female) to assess the effects of *MKX* and *SCX* across different populations. The Sircol collagen kit used to measure total collagen content does not differentiate between collagen types, and thus it is hard to determine whether the protein level changes in collagen are more indicative of outer AF collagen Type I or other collagens such as collagen II in the inner AF. In addition, due to the use of Calcein, a green fluorescent marker, for assessing cell viability in this study, the transfection efficiency of the GFP tags was not assessed and future studies should include an assessment of transfection efficiency along with protein level confirmation of *MKX* and *SCX* to validate the transfection. Lastly, the study was conducted on standard plastic monolayer which may impact cellular morphology without proper ECM alignment structures as native AF tissue. Future studies will incorporate more physiologically relevant substrates such as aligned nanofiber substrates to yield cellular alignment, which has shown to exhibit similar properties as native AF tissue.³⁰

5 | CONCLUSION

This proof-of-concept study demonstrates the potential of AF transcription factors *MKX* or *SCX*, to drive reprogramming of mildly/

moderately degenerate human cadaveric and severely degenerated LBP patient-derived AF cells toward a healthy phenotype, evidenced by the fibroblast-like morphology, upregulation of key transcription factors present in AF tissue, decreased catabolism, increased anabolism of ECM components, with regulation of inflammatory cytokines and pain markers. Nonviral transfection of innate diseased patient cells has greater therapeutic potential compared to viral and cell-based therapies for treatment of IVD-associated LBP. Future studies aim to use engineered EVs to deliver these transcription factors to AF cells with the incorporation of sex/age patient groups and in-vivo animal studies to assess the safety and efficacy of this therapeutic approach.

AUTHOR CONTRIBUTIONS

Shirley Tang, Connor Gantt, Ana Salazar Puerta, and Lucy Bodine performed the experiments and collected data. All authors contributed to the research design, data analysis, data interpretation, drafting, and critical review of the manuscript. All authors have read and approved the final submission of this manuscript.

ACKNOWLEDGMENTS

Financial support for this project was provided by NIH 1R01AR079485-01, NIH R61 AR076786, and the ON/ORS Kickstarter Grant. We thank The Ohio State University Genomics Core and Dr. Sushmitha Durgam for their technical assistance.

CONFLICT OF INTEREST STATEMENT

The authors declare no conflicts of interest. Devina Purmessur is an Editorial Board member of JOR Spine and co-author of this article. They were excluded from editorial decision-making related to the acceptance of this article for publication in the journal.

ORCID

Shirley Tang  <https://orcid.org/0000-0001-8807-2348>

Devina Purmessur  <https://orcid.org/0000-0002-7445-1678>

REFERENCES

- Global Burden of Disease Study 2013 Collaborators, Vos T, Barber RM, et al. Global, regional, and national incidence, prevalence, and years lived with disability for 301 acute and chronic diseases and injuries in 188 countries, 1990–2013: a systematic analysis for the Global Burden of Disease Study 2013. *Lancet*. 2015;386(9995):743-800.
- Katz JN. Lumbar disc disorders and low-back pain: socioeconomic factors and consequences. *J Bone Joint Surg Am*. 2006;88(suppl 2):21-24.
- Freburger JK, Holmes GM, Agans RP, et al. The rising prevalence of chronic low back pain. *Arch Intern Med*. 2009;169(3):251-258.
- Schwarzer AC, Aprill CN, Derby R, et al. The prevalence and clinical features of internal disc disruption in patients with chronic low back pain. *Spine*. 1995;20(17):1878-1883.
- Luoma K, Riihimäki H, Luukkainen R, et al. Low back pain in relation to lumbar disc degeneration. *Spine*. 2000;25(4):487-492.
- Chou R, Qaseem A, Snow V, et al. Diagnosis and treatment of low back pain: a joint clinical practice guideline from the American College of Physicians and the American Pain Society. *Ann Intern Med*. 2007;147(7):478-491.
- Lu Y, Guzman JZ, Purmessur D, et al. Nonoperative management of discogenic back pain. *Spine*. 2014;39(16):1314-1324.
- Zhao L, Manchikanti L, Kaye AD, Abd-Elsayed A. Treatment of discogenic low back pain: current treatment strategies and future options—a literature review. *Curr Pain Headache Rep*. 2019;23(11):86.
- Ghosh P. *The Biology of the Intervertebral Disc*. Vol 2. 1st ed. CRC Press; 1988:39-108.
- Liang T, Zhang L-LL, Xia W, et al. Individual collagen fibril thickening and stiffening of annulus fibrosus in degenerative intervertebral disc. *Spine*. 2017;42(19):E1104-E1111.
- Trout JJ, Buckwalter JA, Moore KC. Ultrastructure of the human intervertebral disc: II. Cells of the nucleus pulposus. *Anat Rec*. 1982;204(4):307-314.
- Yu J, Schollum ML, Wade KR, et al. ISSLS prize winner: A detailed examination of the elastic network leads to a new understanding of annulus fibrosus organization. *Spine*. 2015;40(15):1149-1157.
- Paul R, Haydon RC, Cheng H, et al. Potential use of Sox9 gene therapy for intervertebral degenerative disc disease. *Spine*. 2003;28(8):755-763.
- Martinez-Vaz BM, Makarevitch I, Stensland S. Studying gene expression: database searches and promoter fusions to investigate transcriptional regulation in bacteria. *J Microbiol Biol Educ*. 2010;11(1):42-49.
- Nakamichi R, Ito Y, Inui M, et al. Mohawk promotes the maintenance and regeneration of the outer annulus fibrosus of intervertebral discs. *Nat Commun*. 2016;7(1):1-14.
- Peredo AP, Tsinman TK, Bonnevie ED, et al. Developmental morphogens direct human induced pluripotent stem cells towards an annulus fibrosus-like cell phenotype. *bioRxiv*. 2022. doi:10.1101/2022.05.06.490483
- Torre OM, Mroz V, Benitez ARM, et al. Neonatal annulus fibrosus regeneration occurs via recruitment and proliferation of Scleraxis-lineage cells. *NPJ Regen Med*. 2019;4(1):23.
- Yoshimoto Y, Takimoto A, Watanabe H, et al. Scleraxis is required for maturation of tissue domains for proper integration of the musculoskeletal system. *Sci Rep*. 2017;7(1):45010.
- Freemont AJ. The cellular pathobiology of the degenerate intervertebral disc and discogenic back pain. *Rheumatology*. 2008;48(1):5-10.
- Vergroesen P-P, Kingma I, Emanuel KSS, et al. Mechanics and biology in intervertebral disc degeneration: a vicious circle. *Osteoarthritis Cartilage*. 2015;23(7):1057-1070.
- Pockert AJ, Richardson SM, Le Maitre CL, et al. Modified expression of the ADAMTS enzymes and tissue inhibitor of metalloproteinases 3 during human intervertebral disc degeneration. *Arthritis Rheum*. 2009;60(2):482-491.
- Binch LA, Cole AA, Breakwell LM, et al. Expression and regulation of neurotrophic and angiogenic factors during human intervertebral disc degeneration. *Arthritis Res Ther*. 2014;16(4):416.
- Gorth DJ, Ottone OK, Shapiro IM, Risbud MV. Differential effect of long-term systemic exposure of TNF α on health of the annulus fibrosus and nucleus pulposus of the intervertebral disc. *J Bone Miner Res*. 2020;35(4):725-737.
- Torre OM, Mroz V, Bartelstein MK, et al. Annulus fibrosus cell phenotypes in homeostasis and injury: implications for regenerative strategies. *Ann N Y Acad Sci*. 2019;1442(1):61-78.
- Lin D, Alberton P, Delgado Caceres M, et al. Loss of tenomodulin expression is a risk factor for age-related intervertebral disc degeneration. *Aging Cell*. 2020;19(3):e13091.
- Nakamichi R, Asahara H. The transcription factors regulating intervertebral disc development. *JOR Spine*. 2020;3(1):e1081.
- Nakamichi R, Asahara H. Regulation of tendon and ligament differentiation. *Bone*. 2021;143:115609.
- Tan C, Lui PPY, Lee YW, Wong YM. Scx-transduced tendon-derived stem cells (TDSCs) promoted better tendon repair compared to mock-transduced cells in a rat patellar tendon window injury model. *PLoS One*. 2014;9(5):e97453.

29. Liu H, Zhu S, Zhang C, et al. Crucial transcription factors in tendon development and differentiation: their potential for tendon regeneration. *Cell Tissue Res.* 2014;356(2):287-298.
30. Shamsah AH, Cartmell SH, Richardson SM, Bosworth LA. Tissue engineering the annulus fibrosus using 3D rings of electrospun PCL:PLLA angle-ply nanofiber sheets. *Front Bioeng Biotechnol.* 2020;7:437.
31. Saghari Fard MR, Krueger JP, Stich S, et al. A biodegradable polymeric matrix for the repair of annulus fibrosus defects in intervertebral discs. *Tissue Eng Regen Med.* 2022;19(6):1311-1320.
32. Likhitpanichkul M, Dreischarf M, Illien-Junger S, et al. Fibrin-genipin adhesive hydrogel for annulus fibrosus repair: performance evaluation with large animal organ culture, in situ biomechanics, and in vivo degradation tests. *Eur Cells Mater.* 2014;28:25-38.
33. Sakai D, Mochida J, Iwashina T, et al. Regenerative effects of transplanting mesenchymal stem cells embedded in atelocollagen to the degenerated intervertebral disc. *Biomaterials.* 2006;27(3):335-345.
34. Yoshikawa T, Ueda Y, Miyazaki K, et al. Disc regeneration therapy using marrow mesenchymal cell transplantation. *Spine.* 2010;35(11):E475-E480.
35. Acosta FL, Metz L, Adkisson HD, et al. Porcine intervertebral disc repair using allogeneic juvenile articular chondrocytes or mesenchymal stem cells. *Tissue Eng Part A.* 2011;17(23-24):3045-3055.
36. Orozco L, Soler R, Morera C, et al. Intervertebral disc repair by autologous mesenchymal bone marrow cells: a pilot study. *Transplantation.* 2011;92(7):822-828.
37. Woods N-B, Muessig A, Schmidt M, et al. Lentiviral vector transduction of NOD/SCID repopulating cells results in multiple vector integrations per transduced cell: risk of insertional mutagenesis. *Blood.* 2003;101(4):1284-1289.
38. Sobajima S, Kim JS, Gilbertson LG, Kang JD. Gene therapy for degenerative disc disease. *Gene Ther.* 2004;11(4):390-401.
39. Yarborough M, Sharp RR. Public trust and research a decade later: what have we learned since Jesse Gelsinger's death? *Mol Genet Metab.* 2009;97(1):4-5.
40. Gantenbein B, Tang S, Guerrero J, et al. Non-viral gene delivery methods for bone and joints. *Front Bioeng Biotechnol.* 2020;8:598466.
41. Gallego-Perez D, Pal D, Ghatak S, et al. Topical tissue nano-transfection mediates non-viral stroma reprogramming and rescue. *Nat Nanotechnol.* 2017;12(10):974-979.
42. Ortega-Pineda L, Sunyecz A, Salazar-Puerta AI, et al. Designer extracellular vesicles modulate pro-neuronal cell responses and improve intracranial retention. *Adv Healthc Mater.* 2022;11(5):2100805.
43. Tang S, Richards J, Khan S, et al. Nonviral transfection with brachyury reprograms human intervertebral disc cells to a pro-anabolic anti-catabolic/inflammatory phenotype: a proof of concept study. *J Orthop Res.* 2019;37(11):2389-2400.
44. Tang S, Salazar-Puerta A, Richards J, et al. Non-viral reprogramming of human nucleus pulposus cells with FOXF1 via extracellular vesicle delivery: an in vitro and in vivo study. *Eur Cells Mater.* 2021;41:90-107.
45. Rincon-Benavides MA, Mendonca NC, Cuellar-Gaviria TZ, et al. Engineered vasculogenic extracellular vesicles drive nonviral direct conversions of human dermal fibroblasts into induced endothelial cells and improve wound closure. *Adv Ther.* 2022;6:2200197.
46. Livak KJ, Schmittgen TD. Analysis of relative gene expression data using real-time quantitative PCR and the $2^{-\Delta\Delta CT}$ method. *Methods.* 2001;25(4):402-408.
47. Bruehlmann SB, Rattner JB, Matyas JR, Duncan NA. Regional variations in the cellular matrix of the annulus fibrosus of the intervertebral disc. *J Anat.* 2002;201(2):159-171.
48. Liu YJ, Ren S, Liu YJ, et al. Treatment of rabbit intervertebral disc degeneration with co-transfection by adeno-associated virus-mediated SOX9 and osteogenic protein-1 double genes in vivo. *Int J Mol Med.* 2013;32(5):1063-1068.
49. Du J, Guo W, Häckel S, et al. The function of CD146 in human annulus fibrosus cells and mechanism of the regulation by TGF- β . *J Orthop Res.* 2022;40(7):1661-1671. doi:10.1002/jor.25190
50. Risbud MV, Schoepflin ZR, Mwale F, et al. Defining the phenotype of young healthy nucleus pulposus cells: recommendations of the spine research Interest Group at the 2014 annual ORS meeting. *J Orthop Res.* 2015;33(3):283-293.
51. Minogue BM, Richardson SM, Zeef LAH, et al. Transcriptional profiling of bovine intervertebral disc cells: implications for identification of normal and degenerate human intervertebral disc cell phenotypes. *Arthritis Res Ther.* 2010;12(1):1-20. doi:10.1186/ar2929
52. Smith LJ, Fazzalari NL. The elastic fibre network of the human lumbar annulus fibrosus: architecture, mechanical function and potential role in the progression of intervertebral disc degeneration. *Eur Spine J.* 2009;18(4):439-448.
53. Furukawa T, Ito K, Nuka S, et al. Absence of biglycan accelerates the degenerative process in mouse intervertebral disc. *Spine.* 2009;34(25):E911-E917.
54. Melrose J, Ghosh P, Taylor TKF, et al. Elevated synthesis of biglycan and decorin in an ovine annular lesion model of experimental disc degeneration. *Eur Spine J.* 1997;6(6):376.
55. Le Maitre CL, Freemont AJ, Hoyland JA. The role of interleukin-1 in the pathogenesis of human intervertebral disc degeneration. *Arthritis Res Ther.* 2005;7(4):R732.
56. Vo NV, Hartman RA, Yurube T, et al. Expression and regulation of metalloproteinases and their inhibitors in intervertebral disc aging and degeneration. *J Spine.* 2013;13(3):331-341.
57. Kao TH, Peng YJ, Tsou HK, et al. Nerve growth factor promotes expression of novel genes in intervertebral disc cells that regulate tissue degradation: laboratory investigation. *J Neurosurg Spine.* 2014;21(4):653-661.
58. Purmessur D, Freemont AJ, Hoyland JA. Expression and regulation of neurotrophins in the nondegenerate and degenerate human intervertebral disc. *Arthritis Res Ther.* 2008;10(4):R99.
59. Cho H, Lee S, Park SH, et al. Synergistic effect of combined growth factors in porcine intervertebral disc degeneration. *Connect Tissue Res.* 2013;54(3):181-186.
60. Moon SH, Nishida K, Gilbertson LG, et al. Biologic response of human intervertebral disc cells to gene therapy cocktail. *Spine.* 2008;33(17):1850-1855.
61. Kim DJ, Moon SH, Kim H, et al. Bone morphogenetic protein-2 facilitates expression of chondrogenic, not osteogenic, phenotype of human intervertebral disc cells. *Spine.* 2003;28(24):2679-2684.
62. Hoogendoorn RJW, Helder MN, Kroeze RJ, et al. Reproducible long-term disc degeneration in a large animal model. *Spine.* 2008;33(9):949-954.
63. Chu G, Shi C, Wang H, et al. Strategies for annulus fibrosus regeneration: from biological therapies to tissue engineering. *Front Bioeng Biotechnol.* 2018;6:90.
64. Wallach CJ, Gilbertson LG, Kang JD. Gene therapy applications for intervertebral disc degeneration. *Spine.* 2003;28(suppl):S93-S98.
65. Clouet J, Fusellier M, Camus A, et al. *Intervertebral Disc Regeneration: From Cell Therapy to the Development of Novel Bioinspired Endogenous Repair Strategies.* Elsevier BV; 2019.
66. Kotnik T, Kramar P, Pucihar G, et al. Cell membrane electroporation—part 1: the phenomenon. *IEEE Electr Insul Mag.* 2012;28(5):14-23.
67. Batista Napotnik T, Reberšek M, Vernier PT, et al. Effects of high voltage nanosecond electric pulses on eukaryotic cells (in vitro): a systematic review. *Bioelectrochemistry.* 2016;110:1-12.
68. O'Brien K, Breyne K, Ughetto S, et al. RNA delivery by extracellular vesicles in mammalian cells and its applications. *Nat Rev Mol Cell Biol.* 2020;21(10):585-606.
69. Mosley GE, Wang M, Nasser P, et al. Males and females exhibit distinct relationships between intervertebral disc degeneration and pain in a rat model. *Sci Rep.* 2020;10(1):15120.

70. Machino M, Nakashima H, Ito K, et al. Age-related degenerative changes and sex-specific differences in osseous anatomy and intervertebral disc height of the thoracolumbar spine. *J Clin Neurosci*. 2021;90:317-324.

SUPPORTING INFORMATION

Additional supporting information can be found online in the Supporting Information section at the end of this article.

How to cite this article: Tang, S., Gantt, C., Salazar Puerta, A., Bodine, L., Khan, S., Higuera-Castro, N., & Purmessur, D. (2023). Nonviral overexpression of Scleraxis or Mohawk drives reprogramming of degenerate human annulus fibrosus cells from a diseased to a healthy phenotype. *JOR Spine*, 6(3), e1270. <https://doi.org/10.1002/jsp2.1270>